

# Presynaptic Inhibition Selectively Weakens Peptidergic Cotransmission in a Small Motor System

Nicholas D. DeLong, Mark P. Beenhakker, and Michael P. Nusbaum

Department of Neuroscience, University of Pennsylvania School of Medicine, Philadelphia, Pennsylvania

Submitted 11 September 2009; accepted in final form 12 October 2009

**DeLong ND, Beenhakker MP, Nusbaum MP.** Presynaptic inhibition selectively weakens peptidergic cotransmission in a small motor system. *J Neurophysiol* 102: 3492–3504, 2009. First published October 14, 2009; doi:10.1152/jn.00833.2009. The presence and influence of neurons containing multiple neurotransmitters is well established, including the ability of coreleased transmitters to influence the same or different postsynaptic targets. Little is known, however, regarding whether presynaptic regulation of multitransmitter neurons influences all transmission from these neurons. Using the identified neurons and motor networks in the crab stomatogastric ganglion, we document the ability of presynaptic inhibition to selectively inhibit peptidergic cotransmission. Specifically, we determine that the gastropyloric receptor (GPR) proprioceptor neuron uses presynaptic inhibition to selectively regulate peptidergic cotransmission from the axon terminals of MCN1, a projection neuron that drives the biphasic (retraction, protraction) gastric mill (chewing) rhythm. MCN1 drives this rhythm via fast GABAergic excitation of the retractor neuron Int1 and slow peptidergic excitation of the lateral gastric (LG) protractor neuron. We first demonstrate that GPR inhibition of the MCN1 axon terminals is serotonergic and then establish that this serotonergic inhibition weakens MCN1 peptidergic excitation of LG without altering MCN1 GABAergic excitation of Int1. At the circuit level, we show that this selective regulation of MCN1 peptidergic cotransmission is necessary for the normal GPR regulation of the gastric mill rhythm. This is the first demonstration, at the level of individual identified neurons, that a presynaptic input can selectively regulate a subset of coreleased transmitters. This selective regulation changes the balance of cotransmitter actions by the target multitransmitter neuron, thereby enabling this neuron to have state-dependent actions on its target network. This finding reveals additional flexibility afforded by the ability of neurons to corelease multiple neurotransmitters.

## INTRODUCTION

Cotransmission provides the potential for additional flexibility in neuronal signaling (Burnstock 2004; Seal and Edwards 2006). In general, cotransmission enables the convergence or divergence of coreleased transmitters onto the same or separate target cells, respectively (Blitz and Nusbaum 1999; Dugue et al. 2005; Jan and Jan 1982; Lu et al. 2008; Maher and Westbrook 2008; Nishimaru et al. 2005; Stein et al. 2007; Vilim et al. 2000). At the level of network activity, however, the impact of cotransmission remains largely unexplored (Blitz and Nusbaum 1999; Koh and Weiss 2007; Sun et al. 2003). Even less well understood is whether presynaptic regulation of synaptic transmission can selectively regulate only a subset of coreleased transmitters, thereby revealing another level of network flexibility.

Address for reprint requests and other correspondence: M. P. Nusbaum, Department of Neuroscience, University of Pennsylvania School of Medicine, 215 Stemmler Hall, Philadelphia, PA 19104-6074 (E-mail: nusbaum@mail.med.upenn.edu).

Here we examine the synaptic regulation of cotransmission and its impact on rhythmically active motor circuits (central pattern generators [CPGs]) in the isolated stomatogastric nervous system (STNS) of the crab *Cancer borealis* (Marder and Bucher 2007; Nusbaum and Beenhakker 2002). The STNS includes the paired commissural ganglia (CoGs), oesophageal ganglion (OG), and stomatogastric ganglion (STG). The STG contains the CPGs for the gastric mill (chewing) and pyloric (filtering of chewed food) rhythms, whereas most projection neurons that regulate these rhythms originate in the CoGs (Coleman et al. 1992; Nusbaum et al. 2001).

The gastric mill rhythm driven by the CoG projection neuron called modulatory commissural neuron 1 (MCN1) is well characterized, as is its regulation by the muscle stretch-sensitive, gastropyloric receptor (GPR) sensory neuron (Bartos et al. 1999; Beenhakker et al. 2005; Coleman et al. 1995). In brief, MCN1 elicits the gastric mill rhythm via fast, GABAergic excitation of the retractor CPG neuron Int1 (interneuron 1) and slow, peptidergic excitation of the protractor CPG neuron LG (lateral gastric) (Coleman et al. 1995; Stein et al. 2007; Wood et al. 2000). During the MCN1-elicited gastric mill rhythm, GPR stimulation selectively prolongs the gastric mill retractor phase by presynaptically inhibiting the STG terminals of MCN1 (MCN1<sub>STG</sub>) (Beenhakker et al. 2005). This GPR action results at least partly from its weakening MCN1 peptidergic excitation of the LG neuron (Beenhakker et al. 2005).

Here we determine the relative influence of GPR on the coreleased MCN1 transmitters  $\gamma$ -aminobutyric acid (GABA) and *Cancer borealis* tachykinin-related peptide Ia (CabTRP Ia) during the MCN1-elicited gastric mill rhythm. We first show that GPR uses only one of its three cotransmitters (serotonin) to presynaptically inhibit MCN1<sub>STG</sub> and thus to selectively prolong the gastric mill retractor phase. These GPR actions are suppressed by the serotonin receptor antagonist methiothepin. We then take advantage of this methiothepin-sensitive serotonergic action to show that the GPR inhibition of MCN1<sub>STG</sub> does not alter the MCN1 GABAergic excitation of Int1. This presynaptic inhibition thus selectively weakens the MCN1 peptidergic action on the gastric mill CPG. Last, we show that, at the circuit level, this selective inhibition of peptide cotransmission is necessary for GPR to selectively prolong the gastric mill retractor phase.

## METHODS

### *Animals/preparation*

Male crabs [*C. borealis* (Jonah crabs)] were obtained from Yankee Lobster (Boston, MA) and the Marine Biological Laboratory (Woods Hole, MA) and housed in commercial tanks containing chilled (10°C),

filtered, and recirculated artificial seawater. Before dissection, each crab was anesthetized by packing it in ice for  $\geq 30$  min. Briefly, the foregut was removed from the animal, bisected along the ventral midline, and pinned ventral side down in a silicone elastomer (Sylgard 170; K. R. Anderson, Morgan Hill, CA; WPI, Sarasota, FL) coated glass bowl in chilled *C. borealis* saline. The isolated STNS (see Fig. 1A) was then dissected from the foregut, transferred, and pinned down in a Sylgard 184-coated (K. R. Anderson) petri dish filled with saline ( $10\text{--}12^\circ\text{C}$ ). During each experiment, the STNS was continuously superfused with saline ( $7\text{--}12$  ml/min) via a switching manifold, to enable fast solution changes, and cooled ( $10\text{--}11^\circ\text{C}$ ) with a Peltier device. In all experiments, both CoGs were disconnected from the rest of the STNS by bisecting the inferior oesophageal nerves (*ions*) and superior oesophageal nerves (*sons*) (Fig. 1A).

### Solutions

*C. borealis* saline contained (in mM): 440 NaCl, 26 MgCl<sub>2</sub>, 13 CaCl<sub>2</sub>, 11 KCl, 10 Trizma base, and 5 maleic acid (pH 7.4–7.6). Solutions of all pharmacological agents were dissolved in saline during the experiment for which they were used, including methiothepin (Sigma-Aldrich, St. Louis, MO), serotonin (5-hydroxytryptamine [5-HT]; Sigma-Aldrich), oxotremorine sesquifumerate (OXO; Sigma-Aldrich), and allatostatin III (AST; Gly-Gly-Ser-Leu-Tyr-Ser-Phe-Gly-Leu-NH<sub>2</sub>; Item #87-7-30A; American Peptide, Sunnyvale,

CA). Methiothepin ( $10^{-5}$  M) was applied by superfusion. 5-HT, OXO, and AST were applied by pressure-ejection ( $1\text{--}2$  s,  $4\text{--}8$  psi) from a microelectrode ( $1\text{--}2$  M $\Omega$ ) placed immediately above the desheathed STG neuropil, using a Picospritzer II Microinjector (General Valve, Fairfield, NJ). For coapplications of 5-HT with OXO or AST, the two substances were mixed together and coejected from the same microelectrode.

### Electrophysiology

Standard intracellular and extracellular recording techniques were used in this study (Beenhakker et al. 2005). Briefly, extracellular recordings from identified nerves were obtained by electrically isolating sections of nerves from the bath with a petroleum jelly-based cylindrical compartment (Vaseline; Medical Accessories and Supply Headquarters, Alabaster, AL). One of two stainless-steel electrode wires was placed within this compartment to record action potentials (APs) propagating through the nerve and the second wire was placed in the bath as a reference electrode. The differential signal was recorded, filtered, and amplified with AM Systems (Carlsborg, WA; model 1700) and Brownlee Precision (Santa Clara, CA; model 410) amplifiers. Extracellular stimulation of a nerve was achieved by placing the two extracellular recording wires into a stimulus isolation unit (model SIU5; Astromed/Grass Instruments, West Warwick, RI) controlled by a stimulator (model S88; Astromed/Grass Instruments).

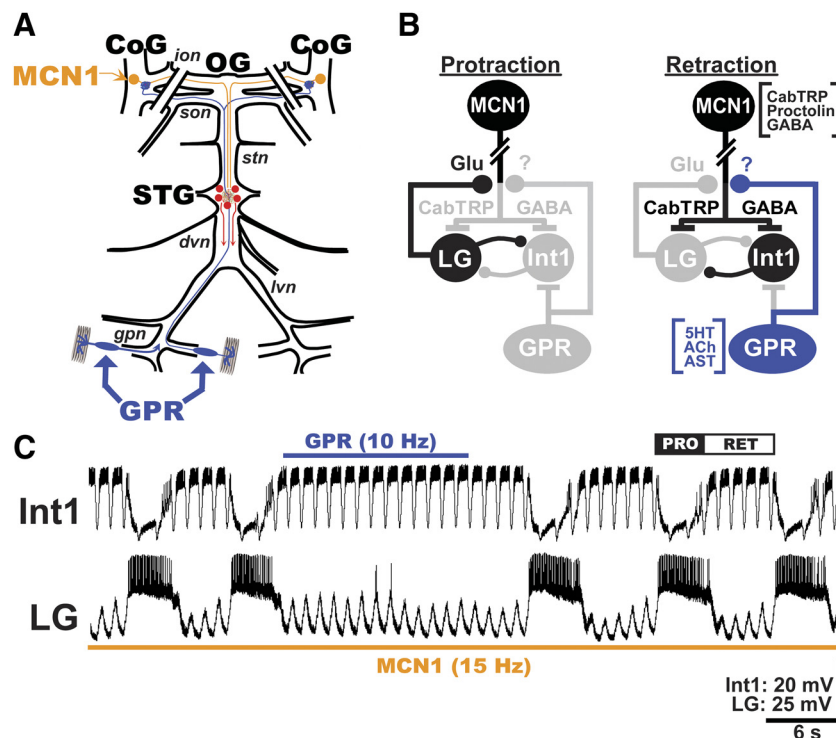


FIG. 1. Schematic of the isolated STNS and MCN1-gastric mill rhythm regulation by the proprioceptor neuron GPR. *A*: in each CoG, there is a single copy of the projection neuron MCN1. MCN1 projects to the STG via the *ion* and *stn* nerves. Each GPR arborizes in the STG and each CoG. The paired diagonal bars through the *sons* and *ions* represent the transection of these nerves at the start of each experiment. Gray rectangles represent protractor muscles in which GPR dendrites arborize. *B*: core gastric mill CPG schematic during each phase (protraction, retraction) of the gastric mill rhythm, including its regulation during retraction by GPR. Paired diagonal bars through MCN1 axon represent additional distance between CoG and STG. All synapses shown are located in the STG neuropil. Gray somata and synapses represent silent neurons/synapses. Synapses drawn on somata or axons actually occur on small branches in the STG neuropil. Note that MCN1 uses only CabTRP Ia to excite LG and only GABA to excite Int1 (Stein et al. 2007; Wood et al. 2000), whereas LG inhibition of MCN1<sub>STG</sub> is mediated by glutamate (Marder 1987; M. J. Coleman and M. P. Nusbaum, unpublished data). The question mark at the GPR-to-MCN1<sub>STG</sub> synapse indicates that, at the start of this project, the GPR transmitter(s) mediating this action was unknown. Symbols: filled circles, synaptic inhibition; *t*-bars, synaptic excitation. MCN1 and GPR cotransmitters are listed alongside their somata. *C*: as shown previously (Beenhakker et al. 2005), GPR stimulation selectively prolongs the retractor phase of the MCN1-elicited gastric mill rhythm. Most hyperpolarized  $V_m$ : Int1,  $-54$  mV; LG,  $-75$  mV. STNS, stomatogastric nervous system; MCN1, modulatory commissural neuron 1; GPR, gastropyloric receptor; STG, stomatogastric ganglion; CoGs, commissural ganglia; CPG, central pattern generator; CabTRP Ia, *Cancer borealis* tachykinin-related peptide Ia; LG, lateral gastric; GABA,  $\gamma$ -aminobutyric acid; Int1, interneuron 1;  $V_m$ , membrane voltage; PRO, protraction; RET, retraction.

Intracellular recordings of STNS somata and axons were obtained with sharp glass microelectrodes (15–30 M $\Omega$ ) filled with 0.6 M K<sub>2</sub>SO<sub>4</sub> plus 20 mM KCl. All intracellular signals were amplified and filtered with Axoclamp 2B amplifiers (Molecular Devices, Sunnyvale, CA) and then further amplified with Brownlee model 410 amplifiers. Intracellular current injections were performed in discontinuous current-clamp (DCC) mode with sampling rates of 2–3 kHz. To facilitate intracellular recordings, the STG was desheathed and viewed with light transmitted through a darkfield condenser (Nikon, Tokyo).

All STNS neurons were identified by their patterns of activity, synaptic interactions with other identified neurons, and axonal branching patterns in connecting and peripheral nerves (Beenhakker et al. 2005; Saideman et al. 2007; Weimann et al. 1991). The gastric mill rhythm was elicited by tonic, extracellular stimulation of the *ion* on the STG side of the bisected nerve (Bartos et al. 1999; Coleman et al. 1995). This nerve contains only two projection neurons that innervate the STG (MCN1, MCN5) and low-intensity *ion* stimulation can selectively activate MCN1 (Bartos and Nusbaum 1997; Coleman and Nusbaum 1994; Coleman et al. 1992; Norris et al. 1996).

GPR stimulation was accomplished by extracellular stimulation of the gastropyloric nerve (*gpn*), through which the GPR2 axon projects (Katz et al. 1998). GPR is present as a pair of bilaterally symmetric neurons (GPR1 and GPR2) that project through different peripheral nerve branches, but their actions on the gastric mill rhythm are equivalent (Beenhakker et al. 2005). Unless otherwise indicated, we stimulated the *gpn* during the retractor phase of the gastric mill rhythm to mimic its likely *in vivo* activity pattern (Beenhakker et al. 2005). This stimulation was performed manually by turning the stimulator on at the beginning of the retractor phase and terminating the stimulation before or immediately after the burst onset time of the LG neuron. LG burst onset marks the end of the retractor phase and the start of the protractor phase.

### Data acquisition and analysis

Data were acquired in parallel onto a chart recorder (Everest model; Astromed) and by digitizing (~5 kHz) and storing the data on computer with data acquisition hardware/software (Spike2; Cambridge Electronic Design, Cambridge, UK). Digitized data were analyzed with a homemade Spike2 program (“The Crab Analyzer”; freely available at <http://www.uni-ulm.de/~wstein/spike2/index.html>). In brief, the burst duration of a neuron was defined as the elapsed time (in seconds) between the first and last AP in an impulse burst. The intraburst firing frequency was calculated by determining the number of APs in a burst minus 1 and then dividing it by the burst duration. The gastric mill cycle period was defined by the duration (in seconds) between the onset of two successive impulse bursts in the LG neuron. All analyses involved determining the mean  $\pm$  SE for the parameter of interest from at least five consecutive gastric mill cycles in each experiment.

Statistical analyses were performed with SigmaStat 3.0 (SPSS, Chicago, IL) or Microsoft Excel (Microsoft, Redmond, WA). Statistical tests used included the paired Student’s *t*-test and repeated-measures (RM) ANOVA. In any case where only two groups were compared, a paired *t*-test was used and the *P* value is reported. Except where noted, all *t*-tests performed were one-tailed. In all other cases, and where noted in the text, an ANOVA was used to compare the precontrol, manipulation (GPR stimulation or neurotransmitter application), and postcontrol groups. For each case, the SigmaStat software was first used to verify a normal distribution (Kolmogorov–Smirnov test). In any case where the ANOVA reported a statistical difference among the compared groups, the Student–Newman–Keuls post hoc test was used and the reported *P* value represents the post hoc comparison of the precontrol and manipulation groups. In all such experiments, the effect of the manipulation was reversible and there was no significant difference between the precontrol and postcontrol

groups. Figures were made from Spike2 files incorporated into Adobe Illustrator and Photoshop (Adobe, San Jose, CA).

### Dynamic clamp

We used the dynamic-clamp technique (Prinz et al. 2004; Sharp et al. 1993) to inject a simulated version of a biological conductance into the LG neuron. Specifically, as in previously published work (Beenhakker et al. 2005), we elicited a gastric mill–like rhythm by injecting into LG a simulated version of the CabTRP Ia–activated conductance. The resulting, voltage-dependent current in LG enables the generation of rhythmic alternating bursts between LG and Int1 that is comparable to those occurring during the MCN1–elicited gastric mill rhythm. These experiments were performed using the version of the dynamic-clamp software developed in the Nadim laboratory (Rutgers University and New Jersey Institute of Technology; available at <http://stg.rutgers.edu/software/>) on a PC running Windows XP and NI PCI-6070-E data acquisition board (National Instruments, Austin, TX). All dynamic-clamp–implemented current injections were performed with intracellular recordings in single-electrode DCC mode.

### Gastric mill model

We implemented a computational model modified as indicated in the following text from an existing conductance-based model of the gastric mill circuit (Beenhakker et al. 2005; Nadim et al. 1998). We retained all aspects of the model implemented by Beenhakker et al. (2005), including modeled versions of the LG, Int1, MCN1, and GPR neurons. The only parameter that was altered from the model version presented in Beenhakker et al. (2005) was the presynaptic voltage dependence of the MCN1 synapse onto Int1. This synapse was modified to increase its sensitivity to GPR inhibition of MCN1 and the results were compared with the original version, as published in Beenhakker et al. (2005). In the modified version, the activation parameter (*m*) for this synapse was modeled as follows

$$m = \frac{1}{1 + e^{-(V+50)}}$$

In the preceding equation, *m* is the activation parameter and *V* is the membrane potential of the MCN1 axon terminal compartment.

## RESULTS

### GPR regulates the MCN1–gastric mill rhythm via serotonin

The MCN1–elicited gastric mill rhythm is a two-phase motor pattern that includes alternating AP bursts in protraction- and retraction-phase STG neurons (Fig. 1) (Saideman et al. 2007). This rhythmic motor activity drives the protraction and retraction chewing movements of the teeth in the gastric mill stomach compartment (Heinzel et al. 1993). In *C. borealis*, the CPG for this rhythm includes the reciprocally inhibitory retractor-phase neuron Int1 and protractor-phase neuron LG, plus MCN1<sub>STG</sub> (Fig. 1B) (Bartos et al. 1999; Coleman et al. 1995).

MCN1 drives the gastric mill rhythm via its slow peptidergic (CabTRP Ia) excitation of LG and fast GABAergic excitation of Int1 (Fig. 1B) (Coleman et al. 1995; Stein et al. 2007; Wood et al. 2000). These MCN1 actions occur during the retraction phase because LG inhibits MCN1<sub>STG</sub> during protraction (Fig. 1B) (Coleman and Nusbaum 1994; Coleman et al. 1995). There are several additional gastric mill motor neurons that are active during the MCN1–gastric mill rhythm, but their activity is not necessary for rhythm generation (Bartos et al. 1999; Saideman et al. 2007).

The GPR neurons are two, bilaterally symmetric pairs of neurons that function as proprioceptors (Katz et al. 1989). Each GPR arborizes its dendrites in protractor muscles that are stretched during the retractor phase of the gastric mill rhythm (Birmingham et al. 1999; Katz et al. 1989). In the isolated STNS, selective extracellular stimulation of either GPR (*gpn* or *mgn* nerves) during the retractor phase of the MCN1–gastric mill rhythm selectively prolongs that phase, due to its presynaptic inhibition of MCN1<sub>STG</sub> (Fig. 1, *B* and *C*) (Beenhakker et al. 2005).

GPR contains the cotransmitters serotonin (5-HT), acetylcholine (ACh), and allatostatin (AST) and it is the only source of 5-HT within the STG (Katz et al. 1989; Skiebe and Schneider 1994). To further elucidate the mechanisms by which GPR regulates the MCN1–gastric mill rhythm, we aimed to determine the role of each GPR cotransmitter in its inhibition of MCN1<sub>STG</sub>.

Relatively brief (1 s), focal application of serotonin ( $10^{-4}$  M) onto the desheathed STG neuropil mimicked the GPR action on the gastric mill rhythm (Fig. 2*A*). Specifically, serotonin application reversibly increased the duration of the subsequent retractor phase (pre-5-HT:  $5.9 \pm 1.0$  s; 5-HT:  $21.8 \pm 5.8$  s; post-5-HT:  $7.6 \pm 2.4$  s;  $n = 7$ ,  $P = 0.009$ ) (Fig. 2*A*). There was no concomitant alteration in the protractor-phase duration (pre-5-HT:  $5.5 \pm 1.4$  s; 5-HT:  $4.7 \pm 1.3$  s; post-5-HT:  $5.6 \pm 1.4$  s;  $n = 7$ ,  $P = 0.87$ ). Similar to our previous results (Beenhakker et al. 2005), GPR stimulation in these same preparations also prolonged the retractor phase (pre-GPR:  $4.8 \pm 0.4$  s; during GPR:  $17.1 \pm 4.8$  s; post-GPR:  $4.9 \pm 0.2$  s;  $n = 4$ ,  $P = 0.022$ ) without altering protraction

duration (pre-GPR:  $4.2 \pm 0.7$  s; during GPR:  $3.6 \pm 0.6$  s; post-GPR:  $4.0 \pm 0.8$  s;  $n = 4$ ,  $P = 0.84$ ) (Fig. 2*B*).

In contrast to these serotonin actions, neither focally applied AST ( $10^{-5}$  M:  $n = 3$ ,  $P = 0.94$ ) nor the muscarinic agonist oxotremorine (OXO:  $10^{-4}$  M:  $n = 3$ ,  $P = 0.94$ ) mimicked the GPR actions on the MCN1–gastric mill rhythm (Fig. 3, *A* and *B*). Similarly, coapplying by pressure ejection from the same micropipette (see METHODS) AST ( $10^{-5}$  M:  $n = 3$ ,  $P = 0.58$ ) or OXO ( $10^{-5}$  M:  $n = 3$ ,  $P = 0.14$ ) with serotonin ( $10^{-4}$  M) was equivalent to applying serotonin alone in the same preparations (Fig. 3, *A* and *B*). We used the muscarinic agonist OXO for these experiments, instead of a nicotinic cholinergic agonist, because the inhibitory response in MCN1<sub>STG</sub> to GPR stimulation appeared to be metabotropic in nature. Specifically, GPR stimulation elicited no unitary inhibitory postsynaptic potentials (IPSPs) in MCN1<sub>STG</sub>, but instead elicited a slow hyperpolarization that outlasted the GPR stimulation (Beenhakker et al. 2005).

To determine whether serotonin was necessary for mediating the GPR actions on the gastric mill rhythm, we tested the ability of the serotonin receptor antagonist methiothepin ( $10^{-5}$  M) to suppress these serotonin and GPR effects. Methiothepin, an antagonist of the 5-HT<sub>2B</sub> receptor in decapod crustaceans (Spitzer et al. 2008), did suppress the influence of pressure-applied serotonin on the gastric mill rhythm. Specifically, methiothepin suppressed the serotonin-mediated prolongation of the gastric mill retractor phase (pre-5-HT:  $8.8 \pm 2.1$  s; 5-HT:  $14.5 \pm 6.0$  s; post-5-HT:  $6.1 \pm 1.6$  s;  $n = 4$ ,  $P = 0.32$ ) (Fig. 2*A*).

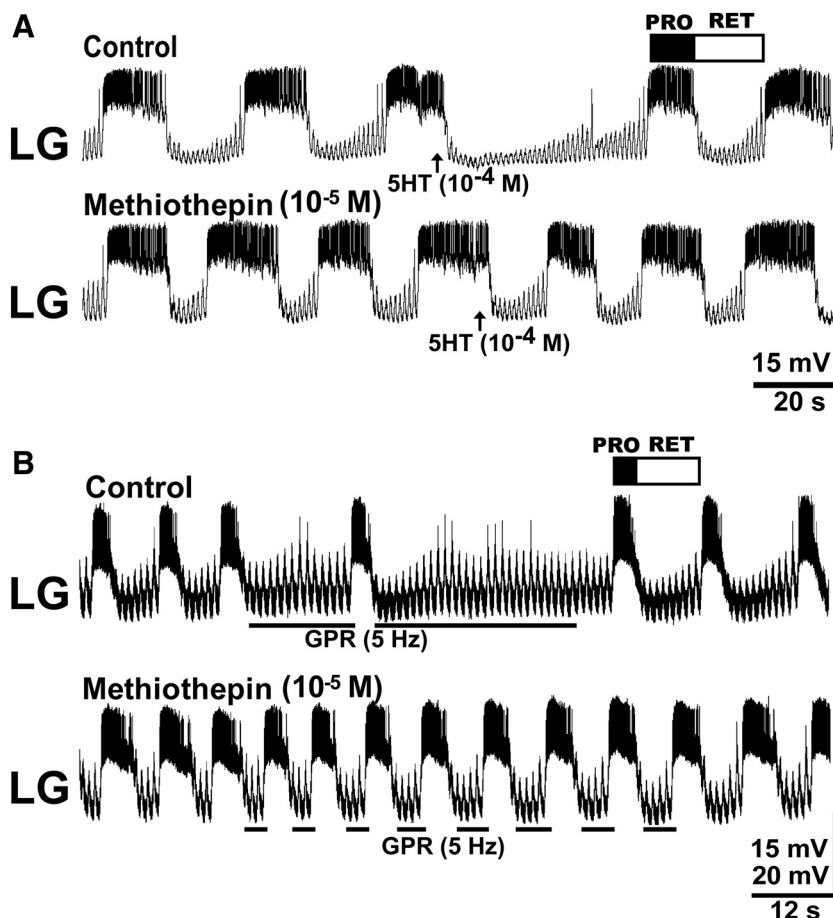


FIG. 2. Regulation of the MCN1-elicited gastric mill rhythm by 5-hydroxytryptamine (5-HT, or serotonin) application and GPR stimulation is suppressed by the serotonin receptor antagonist methiothepin. *A*: bath application of methiothepin suppressed the effect of pressure-ejected 5-HT on the gastric mill rhythm. *Top*: during saline superfusion, brief (1 s) pressure ejection of 5-HT (arrow) onto the desheathed STG neuropil selectively prolonged the gastric mill retractor phase. *Bottom*: during methiothepin superfusion, pressure-ejected 5-HT (arrow) did not alter the gastric mill rhythm. After a 1-h saline wash, 5-HT application again prolonged the retractor phase (not shown). Most hyperpolarized  $V_m$ : LG,  $-63$  mV (in both panels). *B*: bath application of methiothepin suppressed the GPR action on the gastric mill rhythm. *Top*: GPR stimulation (bars) selectively prolonged the retractor phase during normal saline superfusion. *Bottom*: during methiothepin application, GPR stimulation (bars) did not change the retractor-phase duration. After a 1.5-h saline wash, GPR stimulation again prolonged the retractor phase (not shown). Most hyperpolarized  $V_m$ : LG,  $-62$  mV (in both panels). *A* and *B* are from separate preparations.

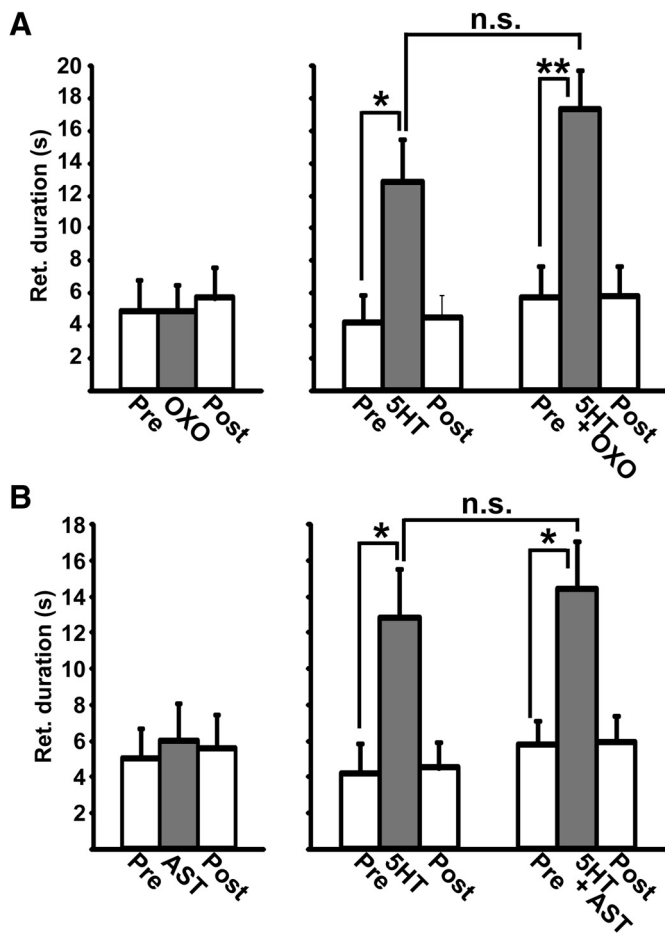


FIG. 3. Serotonin is the only GPR cotransmitter to mimic the ability of GPR stimulation to prolong the retractor phase of the MCN1-elicited gastric mill rhythm. *A, left*: pressure application of the muscarinic agonist oxotremorine (OXO; pipette concentration,  $10^{-4}$  M) to the desheathed STG neuropil did not alter the gastric mill retractor-phase duration relative to the retraction-phase duration pre- and postapplication ( $n = 3$ , repeated-measures [RM]-ANOVA,  $P = 0.94$ ). *Right*: coapplying 5-HT and OXO, from the same microelectrode, prolonged the retractor phase ( $n = 3$ , RM-ANOVA:  $P = 0.01$ ) to the same extent as applying 5-HT alone in the same preparations ( $n = 3$ ,  $P = 0.15$ ). Symbols: n.s., not significant; \* $P < 0.05$ ; \*\* $P < 0.01$ . *B, left*: pressure application of the neuropeptide allatostatin (AST; pipette concentration,  $10^{-5}$  M) did not alter the gastric mill retractor-phase duration relative to the retraction-phase duration pre- and postapplication ( $n = 3$ , RM-ANOVA,  $P = 0.94$ ). *Right*: coapplying 5-HT and AST, from the same microelectrode, also prolonged the retractor phase ( $n = 3$ , RM-ANOVA,  $P = 0.021$ ) to the same extent as 5-HT alone in the same preparations ( $n = 3$ , RM-ANOVA,  $P = 0.58$ ).

Methiothepin also suppressed the GPR influence on the gastric mill rhythm (Fig. 2B). During methiothepin application, GPR stimulation did not change the retractor-phase duration (pre-GPR:  $5.1 \pm 1.0$  s; GPR:  $7.8 \pm 1.2$  s; post-GPR:  $6.6 \pm 1.4$  s;  $n = 5$ ,  $P = 0.32$ ) or the gastric mill cycle period (pre-GPR:  $12.8 \pm 2.7$  s; GPR:  $15.4 \pm 3.4$  s; post-GPR:  $14.0 \pm 3.1$  s;  $n = 5$ ,  $P = 0.86$ ) (Fig. 2B).

In the aforementioned experiments GPR was stimulated only during the behaviorally relevant retractor phase. Insofar as the retractor-phase duration was briefer when GPR was stimulated during methiothepin application, due to the ability of LG to begin its burst sooner, it remained possible that the lack of a GPR-mediated effect during methiothepin application resulted from the relatively brief activation of the GPR pathway and not serotonin receptor blockade. To test this possibility, we took

advantage of the fact that GPR has no effect on the gastric mill rhythm when it is stimulated only during the protraction phase (Fig. 4) and so determined the influence of methiothepin during prolonged, tonic GPR stimulation. During saline superfusion, tonic GPR stimulation still prolonged retraction (pre-GPR:  $4.1 \pm 0.4$  s; during GPR:  $9.3 \pm 1.5$  s,  $n = 5$ ,  $P = 0.01$ ) without altering protraction duration (pre-GPR:  $5.1 \pm 0.9$  s; during GPR:  $3.6 \pm 0.5$  s,  $n = 5$ ,  $P = 0.11$ ), whereas during methiothepin application GPR did not alter retraction (pre-GPR:  $5.4 \pm 0.7$  s; during GPR:  $7.2 \pm 1.3$  s,  $n = 5$ ,  $P = 0.13$ ) or protraction duration (pre-GPR:  $8.3 \pm 1.8$  s; during GPR:  $7.3 \pm 1.7$  s,  $n = 5$ ,  $P = 0.34$ ). These results support the hypothesis that serotonin is pivotal to the GPR regulation of the gastric mill rhythm, with the other GPR cotransmitters playing no apparent role.

#### GPR regulates the gastric mill rhythm via serotonergic inhibition of $MCN1_{STG}$

We hypothesized that methiothepin eliminated the effects of GPR stimulation on the gastric mill rhythm by blocking GPR-mediated inhibition of  $MCN1_{STG}$  (Beenhakker et al. 2005). To test this hypothesis, we took advantage of the fact that GPR stimulation causes a slow hyperpolarization in  $MCN1_{STG}$  that interferes with the ability of  $MCN1$  to initiate APs within the STG in response to depolarizing current injection (Beenhakker et al. 2005). We used this assay to determine whether GPR inhibited  $MCN1_{STG}$  via a methiothepin-sensitive serotonergic synapse.

Pressure-applied 5-HT ( $10^{-4}$  M) mimicked the GPR effects on  $MCN1_{STG}$ , causing  $MCN1_{STG}$  to hyperpolarize and reducing the number of  $MCN1$  APs elicited by each current pulse (pre-5-HT:  $5.6 \pm 1.9$  spikes; during 5-HT:  $0.6 \pm 0.2$  spikes; post-5-HT:  $5.3 \pm 1.8$  spikes; RM-ANOVA,  $P = 0.02$ ,  $n = 5$ ) (Fig. 5A). In these same preparations, GPR stimulation had the same effect (pre-GPR:  $6.1 \pm 2.1$  spikes; during GPR:  $1.3 \pm 0.9$  spikes; post-GPR:  $4.3 \pm 2.2$  spikes; RM-ANOVA,  $P = 0.011$ ,  $n = 4$ ) (Fig. 5B).

Bath-applied methiothepin ( $10^{-5}$  M) prevented the inhibition of  $MCN1_{STG}$  spiking by 5-HT application during depolarizing current injections (pre-5-HT:  $8.8 \pm 0.7$  spikes; during 5-HT:  $7.4 \pm 1.8$  spikes; post-5-HT:  $7.8 \pm 0.8$  spikes; RM-ANOVA,  $P = 0.10$ ,  $n = 5$ ) (Fig. 5A). It also prevented the GPR inhibition of  $MCN1_{STG}$  spiking in response to comparable depolarizations (pre-GPR:  $11.8 \pm 1.7$  spikes; during GPR:  $8.8 \pm 1.5$  spikes; post-GPR:  $11.3 \pm 1.4$  spikes; RM-ANOVA,  $P = 0.06$ ,  $n = 4$ ) (Fig. 5B). These results thus support the hypothesis that GPR inhibits  $MCN1_{STG}$  by a methiothepin-sensitive serotonergic action.

To further test the hypothesis that GPR regulated the gastric mill rhythm exclusively via its inhibition of  $MCN1_{STG}$ , we assessed the GPR influence on a gastric mill-like rhythm elicited by dynamic-clamp current injection. Specifically, in the absence of  $MCN1$  stimulation, we injected into LG a simulated version of the modulator-activated conductance ( $G_{MI-MCN1}$ ) that is normally elicited by  $MCN1$ -released CabTRP Ia and is responsible for driving the gastric mill rhythm (DeLong et al. 2009). This manipulation elicits a gastric mill-like rhythm in LG (Fig. 6), by activating LG in a manner that enables rhythmic reciprocal inhibitory interactions with Int1, which is spontaneously active (Beenhakker et al. 2005).

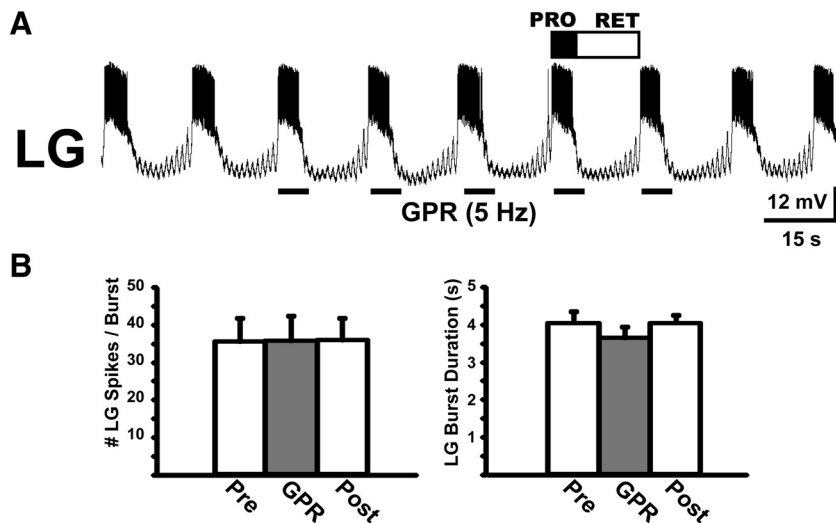


FIG. 4. GPR stimulation during the gastric mill protractor phase did not alter LG activity. *A*: rhythmic GPR stimulation (bars) during protraction did not alter either phase of the MCN1-elicited gastric mill rhythm. Most hyperpolarized  $V_m$ :  $-61$  mV. *B*: across preparations, rhythmic GPR stimulation during protraction did not alter either the number of LG spikes/burst ( $n = 4$ ,  $P = 0.99$ ) or its burst duration ( $n = 4$ ,  $P = 0.49$ ).

When GPR was stimulated during the retractor phase (LG interburst) of the dynamic-clamp-simulated gastric mill rhythm, it did not influence either the LG interburst (retraction) duration (pre-GPR:  $5.7 \pm 0.8$  s; during GPR:  $7.6 \pm 0.7$  s; post-GPR:  $7.2 \pm 0.8$  s;  $P = 0.25$ ,  $n = 5$ ) or its burst (protraction) duration (pre-GPR:  $2.6 \pm 0.6$  s; during GPR:  $2.6 \pm 0.6$  s; post-GPR:  $2.9 \pm 0.6$  s;  $P = 0.96$ ,  $n = 5$ ) (Fig. 6). These data further support the hypothesis that GPR regulates this rhythm exclusively via its serotonergic inhibition of MCN1<sub>STG</sub>.

#### GPR actions on Int1 and LG are methiothepin insensitive

To strengthen the hypothesis that GPR regulates the gastric mill rhythm exclusively via its serotonergic presynaptic inhi-

bitation of MCN1<sub>STG</sub>, we determined whether GPR influenced either Int1 or LG via 5-HT and whether methiothepin influenced the activity of either neuron. GPR APs elicit unitary excitatory postsynaptic potentials (EPSPs) in Int1 (Beenhakker et al. 2005). These EPSPs, however, are unlikely to be mediated by 5-HT because Int1 was unresponsive to pressure-applied 5-HT (Fig. 7, *A* and *B*). It was nonetheless possible that methiothepin altered the Int1 response to GPR stimulation by a nonspecific action. This possibility, however, was not supported by the fact that the GPR excitation of Int1 remained effective in the presence of methiothepin (pre-GPR:  $1.4 \pm 1.0$  Hz; during GPR:  $9.5 \pm 1.2$  Hz;  $n = 5$ ,  $P = 4.1 \times 10^{-4}$ ).

The LG neuron was generally inactive when there was no gastric mill rhythm. At these times no substantial change in its resting potential resulted from either GPR stimulation

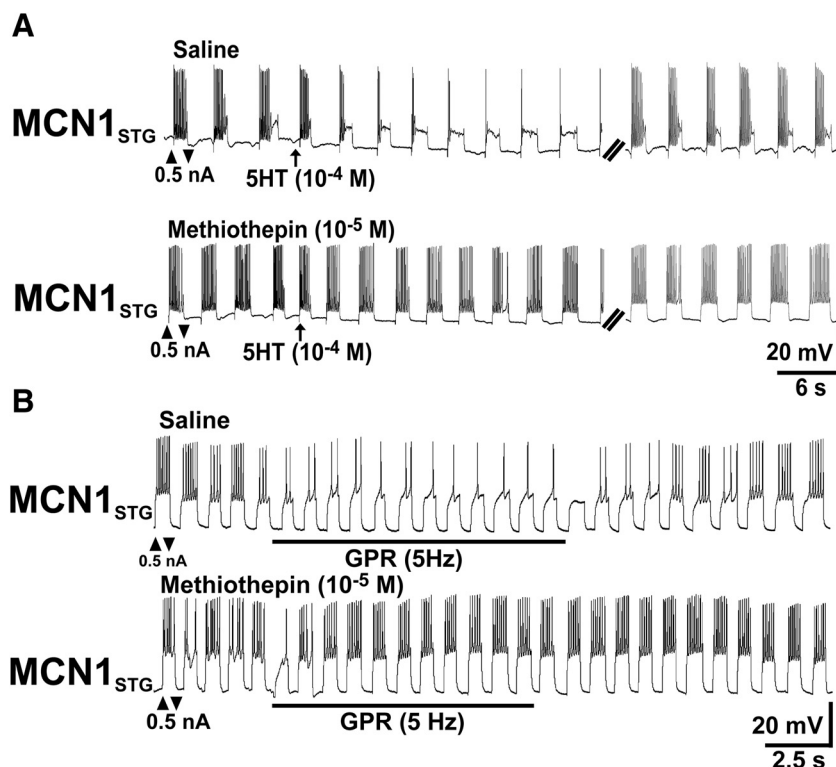


FIG. 5. 5-HT and GPR inhibit MCN1<sub>STG</sub> via a methiothepin-sensitive action. *A*, *top*: the number of MCN1<sub>STG</sub> spikes elicited by rhythmic depolarizing current injections was reduced by 5-HT application (1 s, arrow) onto the desheathed STG neuropil during saline superfusion (pre-5-HT:  $13.2 \pm 0.4$  spikes; steady-state post-5-HT: 1.0 spike;  $n = 5$  cycles). *Bottom*: 5-HT application (1 s, arrow) with methiothepin present had a weaker effect on the MCN1<sub>STG</sub> response to depolarizing current injections than that during saline superfusion (pre-5-HT:  $14.4 \pm 1.8$  spikes; steady-state post-5-HT:  $9.4 \pm 1.2$  spikes;  $n = 5$  cycles). Double hashmarks in each panel represent a time break (10–30 s). Most hyperpolarized  $V_m$ , MCN1<sub>STG</sub>: *top*,  $-62$  mV; *bottom*,  $-63$  mV. *B*, *top*: during rhythmic depolarizing current injections as before, the number of elicited MCN1<sub>STG</sub> spikes was reduced or eliminated during and for a brief time after GPR stimulation (pre-GPR:  $6.2 \pm 0.6$  spikes; during GPR:  $1.3 \pm 0.2$  spikes/dep.;  $n = 5$  cycles). *Bottom*: GPR stimulation did not alter the MCN1<sub>STG</sub> response to these current injections during methiothepin superfusion (pre-GPR:  $5.2 \pm 1.0$  spikes; during GPR:  $6.0 \pm 0.4$  spikes;  $n = 5$  cycles). Most hyperpolarized  $V_m$ , MCN1<sub>STG</sub>: *top*,  $-54$  mV; *bottom*,  $-54$  mV.

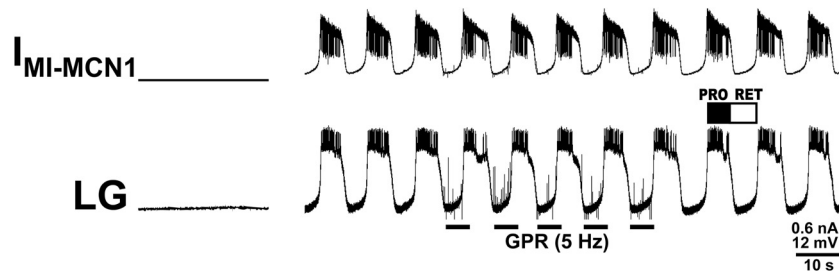


FIG. 6. GPR does not influence the dynamic-clamp-elicited gastric mill-like rhythm. *Left*: prior to activating the dynamic-clamp injections, the LG neuron was silent.  $V_m$ :  $-71$  mV. *Right*: activation of the MCN1-like gastric mill rhythm by dynamic-clamp injection of the modulator (MCN1)-activated voltage-dependent inward current ( $I_{MI-MCN1}$ ) into LG, in the absence of MCN1 stimulation (Beenhakker et al. 2005). During this rhythm, GPR stimulation (bars) during a succession of retractor phases did not alter either phase of the MCN1-like gastric mill rhythm. Note that the  $I_{MI-MCN1}$  injections were regulated both by the voltage-dependent characteristics of the current and by LG burst-timed deactivation to mimic the natural LG presynaptic inhibition of MCN1<sub>STG</sub> (Beenhakker et al. 2005). The LG-mediated deactivation of  $I_{MI-MCN1}$  is evident by the steadily decreasing  $I_{MI-MCN1}$  amplitude during each LG burst. The fast transient events during the LG interbursts represent *gpn* nerve stimulation artifacts. Most hyperpolarized  $V_m$ :  $-75$  mV.

(pre-GPR:  $-63.4 \pm 6.1$  mV; during GPR:  $-63.7 \pm 6.5$  mV,  $n = 5$ ) or 5-HT application (pre-5-HT:  $-59.7 \pm 8.5$  mV; 5-HT:  $-60.9 \pm 9.3$  mV,  $P = 0.10$ ,  $n = 3$ ). However, in the absence of MCN1 stimulation, the number of LG spikes per depolarizing current pulse was reversibly reduced by both GPR stimulation and 5-HT application (Fig. 7, C and D). This GPR action on LG must be mediated by a distinct 5-HT receptor, however, because it persisted in the presence of methiothepin ( $n = 3$ ,  $P = 0.036$ ). Additionally, as shown earlier, this GPR action on LG was ineffective during the gastric mill rhythm, even when GPR was stimulated during the LG burst (Fig. 4).

A previous study also documented both a GPR-elicited EPSP in LG and a post-GPR stimulation increase in the pyloric-timed LG oscillations (Katz and Harris-Warrick 1991). However, we observed these EPSPs in only 2 of  $>50$  preparations and did not observe the increased pyloric-timed oscillations ( $n > 50$ ). Presumably, the distinction between the earlier and current experiments was the conditions under which the recordings were made. In the earlier work there

was minimal background activity in LG and the LG input resistance was presumably relatively high, due to reduced synaptic input, because input from the CoGs and OG was blocked and no projection neurons were stimulated or modulators applied. Under these conditions, the LG membrane potential was generally flat or exhibited small-amplitude pyloric-timed oscillations because there was no gastric mill rhythm and the pyloric rhythm was silent or cycling slowly (Katz and Harris-Warrick 1991). In contrast, during our recordings LG received considerable input from synapses and/or current injection and exhibited relatively large amplitude pyloric- and gastric mill-timed oscillations, which presumably reduced its input resistance and could have shunted the relatively small amplitude EPSPs and obscured the modest pyloric-timed oscillations. Irrespective of whether these events were present (and not observed) or not present in our experiments, they did not have an impact on the results of our GPR stimulations, insofar as eliminating the GPR influence on MCN1<sub>STG</sub> was sufficient to account for the GPR influence on the gastric mill rhythm.

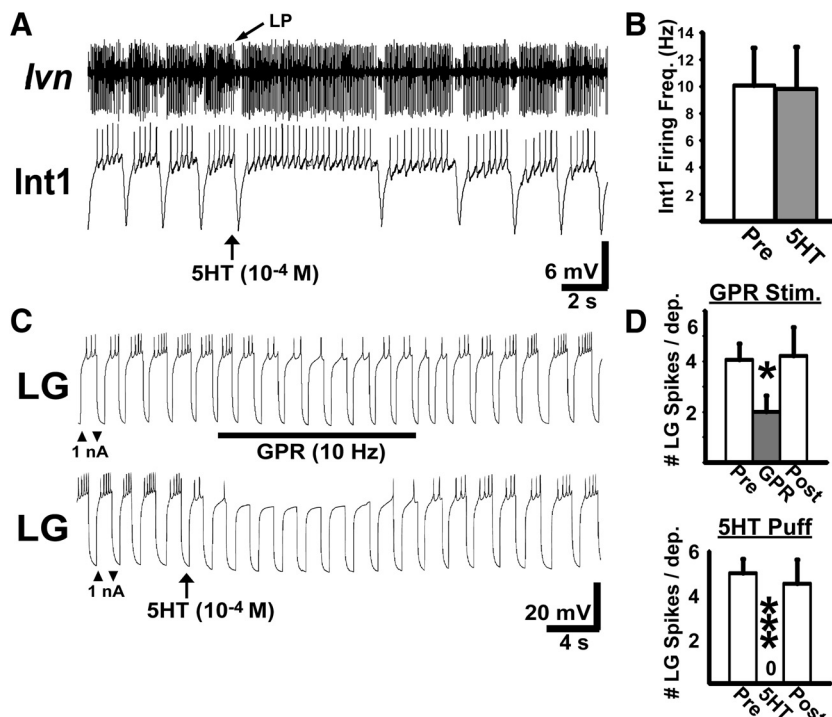


FIG. 7. Focal 5-HT application does not alter Int1 activity but it does inhibit LG activity. *A*: in the absence of a gastric mill rhythm, pressure-ejected 5-HT (1 s, bar) onto the desheathed STG neuropil did not alter the pyloric rhythm-timed intraburst firing frequency of Int1 (pre-5-HT:  $4.3 \pm 0.1$  Hz,  $n = 5$  cycles; 5-HT:  $3.9$  Hz,  $n = 1$  cycle; post-5-HT:  $5.1 \pm 0.2$  Hz,  $n = 5$  cycles). The 5-HT application was effective in that it prolonged the pyloric cycle period (note increased duration of the first lateral pyloric [LP] neuron burst after the 5-HT application). The pyloric rhythm is recorded in the *lvn* (large unit: LP neuron; small unit: pyloric dilator [PD] neuron). Most hyperpolarized  $V_m$ :  $-58$  mV. *B*: 5-HT application did not alter spontaneous Int1 activity across preparations ( $n = 4$ ,  $P = 0.42$ ). *C*: both GPR stimulation and 5-HT application inhibited LG activity driven by rhythmic depolarizing current pulses in LG. *Top*: spikes in LG from each current injection were inhibited by GPR stimulation (pre-GPR:  $5.3 \pm 0.3$  spikes; during GPR:  $1.4 \pm 0.2$  spikes). *Bottom*: depolarization-elicited LG spikes were inhibited by focally applied 5-HT (pre-5-HT:  $4.4 \pm 0.3$  spikes; post-5-HT:  $0$  spikes). Most hyperpolarized  $V_m$ : (both panels)  $-60$  mV. *D*: LG activity was inhibited across preparations by both GPR stimulation (RM-ANOVA,  $P = 0.035$ ,  $n = 3$ ) and 5-HT application (RM-ANOVA,  $P = 0.002$ ,  $n = 3$ ).

*GPR selectively inhibits the MCN1 peptidergic action on the gastric mill CPG*

When GPR is stimulated during a MCN1-elicited gastric mill rhythm, the MCN1 excitation of LG is weakened and its GABAergic excitation of Int1 appears to be unchanged (Beenhakker et al. 2005). This suggested that GPR inhibition of MCN1<sub>STG</sub> reduces CabTRP Ia release but not GABA release, insofar as MCN1 influences LG only via CabTRP Ia and Int1 only via GABA (Fig. 1B) (Stein et al. 2007; Wood et al. 2000). However, it remained possible that the MCN1 firing rate used to elicit the gastric mill rhythm enabled MCN1 to release sufficient GABA to saturate the GABA receptors on Int1. If so, then GPR or 5-HT inhibition of MCN1<sub>STG</sub> may have been insufficient to reduce GABA levels below those that saturate GABA receptors on Int1. Because 5-HT mimicked the GPR effect on MCN1<sub>STG</sub> (Fig. 5) whereas, unlike GPR, it had no direct effect on Int1 (Fig. 7, A and B), we tested the saturation hypothesis by determining whether 5-HT application could weaken Int1 activity during gastric mill rhythms elicited by a lower MCN1 stimulation frequency that caused a submaximal Int1 firing frequency.

As expected, the standard MCN1 stimulation (15–20 Hz) used to drive the gastric mill rhythm increased the Int1 firing rate (pre-MCN1:  $9.9 \pm 2.4$  Hz; during MCN1:  $19.9 \pm 1.4$  Hz,  $n = 4$ ,  $P = 0.003$ ) (Beenhakker et al. 2005). Stimulating MCN1 at a lower rate (10 Hz) in these same preparations still

elicited the gastric mill rhythm and also increased Int1 activity (pre-MCN1:  $9.9 \pm 2.4$  Hz; during 10-Hz MCN1 stimulation [Stim.]:  $15.9 \pm 1.8$  Hz;  $n = 4$ ,  $P = 0.007$ ). However, the increased Int1 firing rate during the latter condition was smaller than that during the faster (15–20 Hz) MCN1 stimulation frequency ( $n = 4$ ,  $P = 0.012$ ). Nonetheless, during weaker MCN1 stimulation (7.5–10 Hz), 5-HT application did not reduce the Int1 firing frequency (pre-5-HT:  $15.4 \pm 1.8$  Hz; 5-HT:  $14.8 \pm 1.5$  Hz;  $P = 0.39$ ,  $n = 4$ ), despite still selectively prolonging the retractor phase (Fig. 8A). Thus it was unlikely that excess GABA release by MCN1 was masking a reduction of its release during the serotonergic inhibition of MCN1<sub>STG</sub> by GPR.

The sensitivity of our assay for GABA release was limited by the relatively high activity level in MCN1 and Int1 during the gastric mill and pyloric rhythms. Therefore we also assayed the ability of 5-HT to regulate MCN1-mediated GABAergic excitation of Int1 with these rhythms silenced and with Int1 maintained at a hyperpolarized membrane potential ( $-70$  mV) to suppress its spontaneous firing. Under these conditions, MCN1 stimulation (2 Hz) did not elicit the gastric mill rhythm but still elicited unitary EPSPs in Int1 (Fig. 8B) (Coleman et al. 1995). Focally applying 5-HT did not alter the amplitude of these EPSPs (pre-5-HT:  $0.74 \pm 0.19$  mV; during 5-HT:  $0.80 \pm 0.16$  mV,  $P = 0.82$ ,  $n = 4$ ) (Fig. 8B). As a positive control for the effectiveness of the 5-HT applications in these prepara-

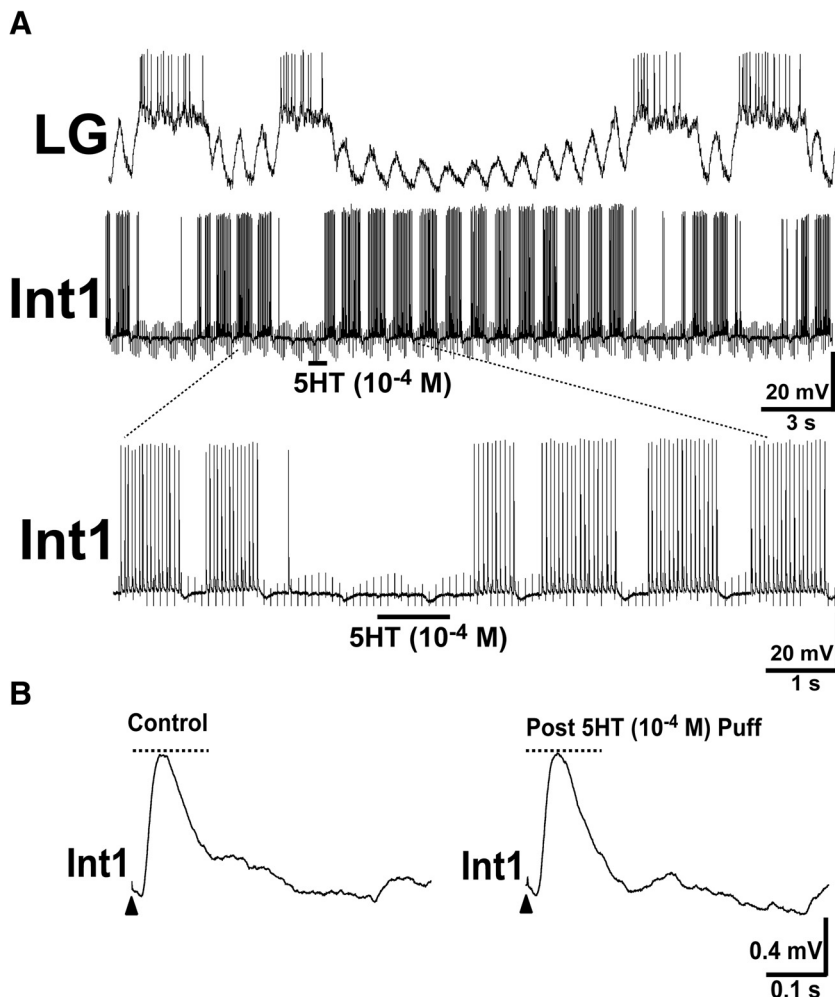


FIG. 8. 5-HT application does not alter MCN1 excitation of Int1. *A, top:* to determine whether GPR stimulation reduced the amount of MCN1<sub>STG</sub>-released GABA, but the effect was masked by stimulating MCN1 at frequencies (15–20 Hz) that saturated the GABA receptors on Int1, 5-HT was pressure-ejected onto the STG neuropil when MCN1 was stimulated at a lower frequency that did not maximally excite Int1. During a gastric mill rhythm elicited by modest MCN1 stimulation (10 Hz), 5-HT application (1 s, bar) did not alter Int1 firing frequency (pre-5-HT:  $18.3 \pm 1.4$  Hz; post-5-HT:  $17.8 \pm 0.2$  Hz), despite still selectively prolonging the gastric mill retractor phase. In this same experiment, increased MCN1 stimulation (20 Hz) elicited a faster Int1 firing rate ( $21.9 \pm 0.3$  Hz). *Bottom:* expanded timescale of a section from A (dotted lines) showing the unchanged Int1 firing frequency after 5-HT application (bar). The fast transient events in Int1 represent *ion* nerve stimulation artifacts. Most hyperpolarized  $V_m$ : Int1,  $-58$  mV; LG,  $-58$  mV. *B:* 5-HT application does not alter the MCN1-elicited excitatory postsynaptic potential (EPSP) amplitude in Int1. During low-frequency MCN1 stimulation (2 Hz), with no gastric mill rhythm elicited and the pyloric rhythm suppressed, MCN1-elicited EPSPs in Int1 were comparable (*left*) without and (*right*) with pressure-ejected 5-HT. Dotted line indicates peak of control EPSP.  $V_{rest}$  (*left, right*):  $-70$  mV. Each record is the average of 10 individual EPSPs.

tions, 5-HT was also applied during the MCN1 (15–20 Hz)-elicited gastric mill rhythm, where it prolonged the retractor phase ( $P = 0.026$ ,  $n = 4$ ) without altering the Int1 firing rate ( $P = 0.15$ ,  $n = 4$ ).

*Selective inhibition of MCN1<sub>STG</sub> peptidergic cotransmission is pivotal to GPR regulation of the gastric mill rhythm*

We tested whether the inability of GPR to alter Int1 activity was necessary for the GPR influence on the gastric mill rhythm. We first evaluated this hypothesis by using a previously described computational model of the GPR-regulated gastric mill rhythm (Beenhakker et al. 2005). Specifically, we simulated the gastric mill rhythm generated by a model gastric mill circuit in which MCN1-mediated peptidergic excitation of LG was selectively reduced by GPR (i.e., MCN1-mediated GABAergic excitation of Int1 was not altered by GPR). We then compared the output of this model to the modified version in which GPR concomitantly reduced MCN1 excitation of both LG and Int1 (Fig. 9).

Consistent with previous work, GPR stimulation prolonged the retractor phase when MCN1-mediated excitation of Int1 persisted (pre-GPR: 7.1 s; GPR: 47.4 s; post-GPR: 9.4 s) without altering the protractor-phase duration (pre-GPR: 10.6 s; GPR: 9.8 s; post-GPR: 10.4 s) (Fig. 9A). The prolonged retractor phase results from GPR inhibition of MCN1<sub>STG</sub>, which reduces the rate of buildup of MCN1 excitation of LG. Due to this reduction, there is an increased duration needed for the CabTRP Ia-activated conductance ( $G_{MI-MCN1}$ ) in LG to

rise to the level needed to overcome Int1 inhibition and enable an LG burst.

We compared the aforementioned model to one in which MCN1 excitation of Int1 was suppressed by GPR inhibition of MCN1<sub>STG</sub> (Int1 spikes/burst: pregastric mill rhythm, five spikes; during gastric mill control cycles, seven spikes; gastric mill cycles with GPR stimulation, five spikes) (Fig. 9B). In this latter model, GPR stimulation produced a 60% increase in retraction-phase duration (pre-GPR: 5.8 s; GPR: 9.8 s; post-GPR: 6.3 s). This change is modest compared with the nearly fivefold increase observed in the original model and the nearly fourfold increase observed experimentally.

The weakened GPR effect on retraction duration in the modified model occurred because the reduced rate of buildup of  $G_{MI-MCN1}$  in LG was paralleled by a weaker Int1 inhibition of LG. Because GPR stimulation reduced Int1-to-LG inhibition in this model, the strength of MCN1-to-LG excitation required for LG to reach burst threshold was decreased (Fig. 9). Similarly, because the modulator-activated conductance was smaller in magnitude than that in control cycles at LG burst onset, less time was needed for this conductance to decay to the level at which the LG burst terminated, thereby reducing the LG burst duration (Fig. 9).

We next used the biological preparation to assess the model prediction that selective inhibition of MCN1 peptidergic cotransmission is necessary for the GPR influence on the gastric mill rhythm. To mimic a hypothetical circuit in which GPR reduced MCN1 excitation of Int1 as well as LG, during the period of GPR stimulations Int1 was injected with sufficient

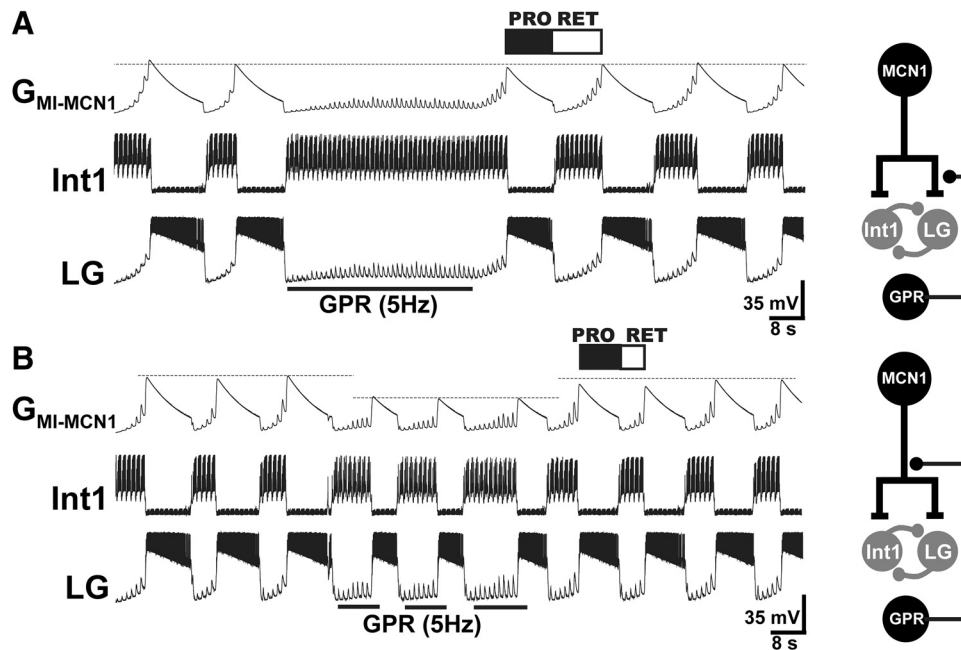


FIG. 9. Selective inhibition of MCN1 peptidergic cotransmission by GPR is necessary for the normal GPR regulation of the MCN1–gastric mill rhythm in a computational model. In this model, MCN1 activates modulator-activated conductance ( $G_{MI-MCN1}$ ) in the LG neuron (Beenhakker et al. 2005). During retraction,  $G_{MI-MCN1}$  steadily builds up until it reaches a level sufficient for LG to escape from Int1 inhibition and burst. During protraction, LG inhibition of MCN1<sub>STG</sub> causes the  $G_{MI-MCN1}$  amplitude to decay until the LG burst terminates. *A, left:* in the biologically realistic model, where GPR inhibition of MCN1<sub>STG</sub> did not alter MCN1 excitation of Int1, GPR stimulation (bar) selectively prolonged the retractor phase. Because GPR did not alter the Int1 firing frequency, the Int1 inhibition of LG was unaffected by GPR. Thus the  $G_{MI-MCN1}$  amplitude needed to overcome this Int1 inhibition was unchanged. The only difference was that during GPR stimulation more time was needed for  $G_{MI-MCN1}$  to reach LG burst threshold (dotted line). *Right:* circuit schematic implemented in this model, with the GPR synapse onto MCN1<sub>STG</sub> being restricted to influencing the MCN1 synapse onto LG and Int1. Symbols: *t*-bars, synaptic excitation; filled circles, synaptic inhibition. *B, left:* in an altered model where GPR inhibition of MCN1 did suppress MCN1 excitation of Int1, GPR stimulation (bars) had a reduced effect on retraction, as well as reducing protraction duration. Note the reduced  $G_{MI-MCN1}$  amplitude that enabled LG burst onset during GPR stimulation (dotted line). *Right:* circuit schematic implemented in this model, showing that the GPR synapse onto MCN1<sub>STG</sub> influenced the MCN1 synapses onto LG and Int1.

constant-amplitude hyperpolarizing current (0.3–0.8 nA) to modestly reduce its firing frequency (during MCN1:  $17.3 \pm 0.8$  Hz; during MCN1 w/GPR and Int1 hyperpolarization [hype.]:  $14.0 \pm 1.2$  Hz;  $n = 4$ , paired  $t$ -test,  $P = 0.012$ ) (Fig. 10).

Consistent with the model prediction, reducing Int1 activity while stimulating GPR altered the GPR influence on the gastric mill rhythm. Instead of selectively prolonging retraction, the retractor-phase duration was unchanged relative to control cycles (Control:  $5.2 \pm 2.0$  s; GPR Stim. plus Int1 hype.:  $6.3 \pm 3.1$  s;  $n = 4$ ,  $P = 0.38$ ) (Fig. 10A). In these same preparations, when Int1 was not hyperpolarized by current injection, retraction was prolonged by GPR stimulation (Control:  $5.2 \pm 2.0$  s; GPR Stim.:  $21.7 \pm 5.5$  s;  $n = 4$ ,  $P = 0.01$ ) (Fig. 10B). Combining GPR stimulation with reduced Int1 activity also did not alter the protractor-phase duration (Control:  $3.5 \pm 1.1$  s; GPR Stim. plus Int1 hype.:  $2.1 \pm 0.3$  s;  $n = 4$ ,  $P = 0.12$ ), as was also the case, as usual, when GPR was stimulated without manipulating Int1 activity (Control:  $3.5 \pm 1.1$  s; GPR Stim.:  $3.5 \pm 1.2$  s;  $n = 4$ ,  $P = 0.48$ ).

## DISCUSSION

We have established that presynaptic inhibition can regulate peptidergic (CabTRP Ia) cotransmission without altering cotransmission mediated by a small-molecule transmitter (GABA). Additionally, because the cotransmitting neuron uses CabTRP Ia and GABA to excite separate postsynaptic neurons, this presynaptic inhibition changes the balance of excitation to the separate postsynaptic targets (Fig. 11). At the circuit level, this regulation of peptidergic cotransmission from the projection neuron

MCN1 is necessary for the proprioceptor GPR to selectively prolong the gastric mill retractor phase. Previous pharmacological studies analyzing bulk release from stimulated sympathetic nerves also support the hypothesis that presynaptic receptors can separately regulate coreleased transmitters (Donoso et al. 2006).

We established that GPR did not weaken MCN1 GABAergic excitation of Int1 by showing that application of the GPR cotransmitter 5-HT mimicked the ability of GPR stimulation to selectively prolong retraction without altering the Int1 firing frequency. This conclusion was strengthened by our findings that 5-HT application neither directly influenced Int1 nor did it alter the MCN1-elicited EPSP amplitude in Int1. We used this approach because GPR is the only source of 5-HT in the STG (Katz et al. 1989) and we determined that the GPR action on MCN1 was serotonergic. We found no evidence that the GPR actions on LG and Int1 contribute to its regulation of the MCN1–gastric mill rhythm (Fig. 11). These GPR synapses, however, may contribute to its regulation of other versions of this rhythm, particularly those in which MCN1 does not participate (e.g., Saideman et al. 2007).

### Selective regulation of peptidergic cotransmission

The intracellular mechanism by which GPR selectively regulates peptidergic cotransmission by MCN1 remains to be determined, although our results suggest that GPR reduces neuropeptide release from MCN1 while sparing GABA release. However, we did not determine how GPR influences the actions of the other MCN1 peptide cotransmitter, proctolin (Blitz et al. 1999), so it remains possible that the serotonergic

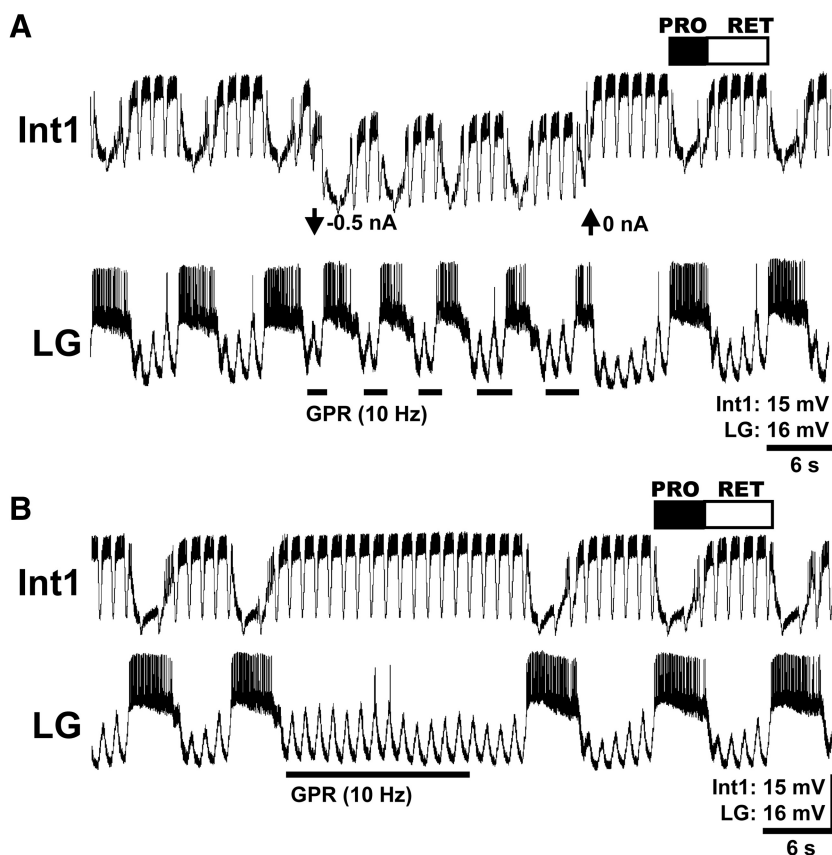


FIG. 10. An unchanging Int1 firing frequency is necessary for the normal GPR regulation of the MCN1–gastric mill rhythm in the biological preparation. *A*: during the gastric mill rhythm, coordinately stimulating GPR (bars) and injecting hyperpolarizing current into Int1 to reduce its firing frequency (pre-GPR/Int1 hyperpolarization [hype.]:  $18.1 \pm 0.1$  Hz; During GPR/Int1 hype.:  $15.8 \pm 0.2$  Hz,  $n = 5$  cycles,  $P = 0.002$ ) did not prolong the retractor phase (pre-GPR/Int1 hype.:  $3.9 \pm 0.1$  s; during GPR/Int1 hype.:  $3.5 \pm 0.4$  s,  $n = 5$  cycles,  $P = 0.19$ ) and reduced the protractor-phase duration (pre-GPR/Int1 hype.:  $2.9 \pm 0.1$  s; during GPR/Int1 hype.:  $1.8 \pm 0.1$  s,  $n = 5$  cycles,  $P = 8.5 \times 10^{-5}$ ). *B*: in the same preparation, GPR stimulation (bar) in the absence of current injection into Int1 selectively prolonged the retractor phase without altering Int1 firing frequency (pre-GPR:  $17.3 \pm 0.7$  Hz; during GPR:  $17.7 \pm 0.3$  Hz,  $n = 5$  cycles,  $P = 0.11$ ). Most hyperpolarized  $V_m$ : LG,  $-65$  mV; Int1,  $-54$  mV.

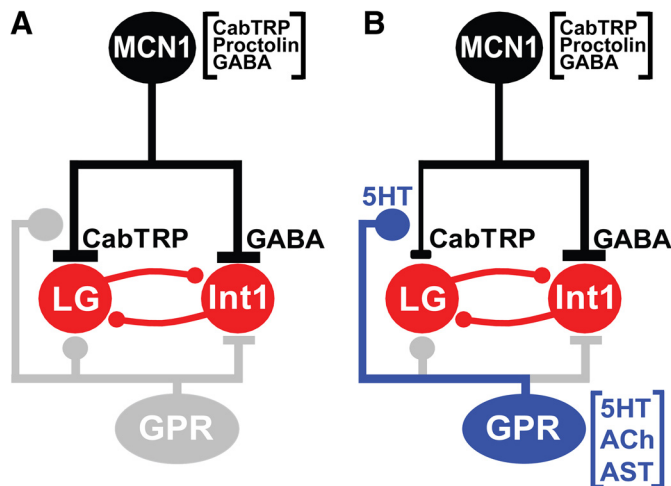


FIG. 11. Summary circuit schematics representing the pathway by which an identified stretch-sensitive proprioceptor neuron (GPR) selectively inhibits peptidergic cotransmission from a modulatory projection neuron (MCN1) that drives a rhythmically active motor circuit. *A*: circuit schematic representing the MCN1 influence on the gastric mill CPG neurons LG and Int1 in the absence of GPR input. *B*: circuit schematic indicating the selectively weakened peptidergic MCN1 synapse onto the LG neuron when GPR is active, as represented by the thinned lines and shortened *t*-bar for the peptidergic synapse. Additionally, this GPR action is mediated by only one GPR cotransmitter (5-HT). Note that the other 2 GPR synapses (gray) onto the gastric mill CPG do not influence this circuit during the MCN1-elicited gastric mill rhythm. Separate transmitter release sites for GABA and CabTRP Ia in MCN1<sub>STG</sub> are shown for diagrammatic purposes only, to represent their separate actions onto Int1 and LG, respectively. There is no available information regarding their sites of release from the MCN1<sub>STG</sub> terminals. The third MCN1 cotransmitter (proctolin) does not influence the gastric mill CPG.

inhibition of MCN1<sub>STG</sub> specifically inhibits CabTRP Ia transmission.

Selective inhibition of neuropeptide release might result from any of several mechanisms. For example, the release sites of GABA and CabTRP Ia may be spatially separated such that the GPR synapse onto MCN1<sub>STG</sub> affects only peptide release, although there is no evidence for spatial segregation of the MCN1<sub>STG</sub> cotransmitters (Blitz et al. 1999; Kilman and Marder 1996). Alternatively, there may be distinct biochemical regulation of neuropeptide and GABA release in MCN1<sub>STG</sub>. Although the molecular-level details underlying neuropeptide release and its regulation lag relative to available information for small-molecule transmitter release, it is clear that there are both shared and distinct aspects to their regulation (de Jong and Verhage 2009; Gracheva et al. 2007; Hammarlund et al. 2008; Sieburth et al. 2007; Speese et al. 2007). Neuropeptide and small-molecule transmitter release also have different intraterminal Ca<sup>2+</sup> requirements and appear to be regulated in at least some terminals by different types of Ca<sup>2+</sup> channels (Ghijssen and Leenders 2005; Ohnuma et al. 2001; Peng and Zucker 1993).

Consistent with the possibility of a biochemical regulation is the likelihood that the GPR inhibition of MCN1<sub>STG</sub> is metabotropic. For example, no unitary IPSPs are recorded in MCN1<sub>STG</sub> in response to GPR stimulation and the resulting hyperpolarization outlasts the GPR stimulation (Beenhakker et al. 2005; this study). Additionally, GPR has metabotropic 5-HT actions on other STG targets (Kiehn and Harris-Warrick 1992) and a G-protein-coupled methiothepin-sensitive 5-HT receptor has

been cloned and characterized in the decapod crustacean nervous system (Spitzer et al. 2008).

The ability of axo-axonic synapses to regulate transmitter release is well documented (Fink and Gothert 2007; Rudomin 2009; Watson et al. 2005), but the effectiveness of these synapses for coregulating the release of multiple transmitters has yet to be explored in other systems. It may well be the case that at a particular set of axon terminals, some presynaptic inputs coregulate the release of all cotransmitters, whereas other inputs target the release of only one or a subset of them. For example, MCN1<sub>STG</sub> receives additional presynaptic inputs, such as from the LG neuron (Coleman and Nusbaum 1994). Thus it will be informative to learn whether the selective regulation of peptide cotransmitter release is a necessary consequence of the organization of the MCN1<sub>STG</sub> axon terminals or whether different presynaptic inputs to MCN1<sub>STG</sub> regulate peptide and GABA release in a manner distinct from GPR.

A changing balance of cotransmitter actions can also result from changes in the firing frequency of a neuron with peptide and small-molecule cotransmitters. Specifically, some cotransmitter neurons have primarily or exclusively small-molecule transmitter-mediated ionotropic synaptic actions when firing at low frequencies, with their metabotropic, peptidergic actions becoming prominent at faster firing frequencies (Peng and Zucker 1993; Vilim et al. 2000). Although this may also be the case for MCN1, it does have peptidergic actions at firing frequencies that are below the frequency threshold for activating the gastric mill rhythm (Kirby and Nusbaum 2007). This distinction between the firing frequency threshold for peptide release and the threshold for the behaviorally relevant firing frequency of a neuron also occurs for at least some other multitransmitter neurons (Vilim et al. 2000).

#### Regulation of network activity by cotransmission

The functional consequences of cotransmitter actions are most extensively studied on individual target cells (Jan and Jan 1982; Lamotte d'Incamps and Ascher 2008; Lu et al. 2008; Maher and Westbrook 2008; Seal and Edwards 2006). However, cotransmission studies have focused on neuronal circuits in *Aplysia* (Koh and Weiss 2007; Koh et al. 2003), rodent thalamus (Brill et al. 2007; Sun et al. 2003), and the STNS (Blitz and Nusbaum 1999; Blitz et al. 1999; Nusbaum et al. 2001; Stein et al. 2007; Thirumalai and Marder 2002; Wood and Nusbaum 2002). It remains to be determined whether presynaptic input selectively regulates peptidergic cotransmission in each of these systems. Where it does occur, its impact is likely to further extend the flexibility already established for neuronal circuits resulting from their modulatory inputs.

Although most cotransmission studies have focused on the convergent actions of coreleased transmitters on a target cell (Koh and Weiss 2007; Koh et al. 2003; Lamotte d'Incamps and Ascher 2008; Lu et al. 2008; Maher and Westbrook 2008; Seal and Edwards 2006), divergent cotransmission has also been documented (Blitz and Nusbaum 1999; Dugue et al. 2005; Nishimaru et al. 2005; Stein et al. 2007; Sun et al. 2003; Thirumalai and Marder 2002; Wood et al. 2000). The ability of GPR to use only one cotransmitter (serotonin) to regulate the MCN1-activated gastric mill CPG extends the influence of divergent cotransmission to sensorimotor integration.

In conclusion, the proprioceptor GPR regulates the MCN1-elicited gastric mill rhythm via a single cotransmitter (serotonin) that selectively regulates peptidergic cotransmission by MCN1<sub>STG</sub>. The distinct regulation of coreleased transmitters by a presynaptic input provides the opportunity for functional compartmentalization, such that arborizations of the cotransmitting neuron in other regions of the CNS would be unaffected by this local regulation. Additionally, as shown here, the altered balance of cotransmitter actions resulting from presynaptic inhibition can change network output without evident changes in either the firing rate or the pattern of the cotransmitting neuron or parallel changes in the modulatory state of the network.

## ACKNOWLEDGMENTS

We thank D. M. Blitz for helpful discussions and comments on earlier versions of this manuscript.

Present address of M. P. Beenhakker: Department of Neurology, Stanford University School of Medicine, Stanford, CA 94305.

## GRANTS

This work was supported by National Institute of Neurological Disorders and Stroke Grants R01-NS-42813 to M. P. Nusbaum, F31-NS-58013 to N. D. DeLong, and F31-NS-41894 to M. P. Beenhakker.

## REFERENCES

- Bartos M, Manor Y, Nadim F, Marder E, Nusbaum MP. Coordination of fast and slow rhythmic neuronal circuits. *J Neurosci* 19: 6650–6660, 1999.
- Bartos M, Nusbaum MP. Intercircuit control of motor pattern modulation by presynaptic inhibition. *J Neurosci* 17: 2247–2256, 1997.
- Beenhakker MP, DeLong ND, Saideman SR, Nadim F, Nusbaum MP. Proprioceptor regulation of motor circuit activity by presynaptic inhibition of a modulatory projection neuron. *J Neurosci* 25: 8794–8806, 2005.
- Birmingham JT, Szuts ZB, Abbott LF, Marder E. Encoding of muscle movement on two timescales by a sensory neuron that switches between spiking and bursting modes. *J Neurophysiol* 82: 2786–2797, 1999.
- Blitz DM, Christie AE, Coleman MJ, Norris BJ, Marder E, Nusbaum MP. Different proctolin neurons elicit distinct motor patterns from a multifunctional neuronal network. *J Neurosci* 19: 5449–5463, 1999.
- Blitz DM, Nusbaum MP. Distinct functions for cotransmitters mediating motor pattern selection. *J Neurosci* 19: 6774–6783, 1999.
- Brill J, Kwakye G, Huguenard JR. NPY signaling through Y1 receptors modulates thalamic oscillations. *Peptides* 28: 250–256, 2007.
- Burnstock G. Cotransmission. *Curr Opin Pharmacol* 4: 47–52, 2006.
- Coleman MJ, Meyrand P, Nusbaum MP. A switch between two modes of synaptic transmission mediated by presynaptic inhibition. *Nature* 378: 502–505, 1995.
- Coleman MJ, Nusbaum MP. Functional consequences of compartmentalization of synaptic input. *J Neurosci* 14: 6544–6552, 1994.
- Coleman MJ, Nusbaum MP, Cournil I, Claiborne BJ. Distribution of modulatory inputs to the stomatogastric ganglion of the crab, *Cancer borealis*. *J Comp Neurol* 325: 581–594, 1992.
- de Jong AP, Verhage M. Presynaptic signal transduction pathways that modulate synaptic transmission. *Curr Opin Neurobiol* 19: 245–253, 2009.
- DeLong ND, Kirby MS, Blitz DM, Nusbaum MP. Parallel regulation of a modulator-activated current via distinct dynamics underlies co-modulation of motor circuit output. *J Neurosci* 29: 12355–12367, 2009.
- Donoso MV, Aedo F, Huidobro-Toro JP. The role of adenosine A<sub>2A</sub> and A<sub>3</sub> receptors on the differential modulation of norepinephrine and neuropeptide Y release from peripheral sympathetic nerve terminals. *J Neurochem* 96: 1680–1695, 2006.
- Dugue GP, Dumoulin A, Triller A, Dieudonne S. Target-dependent use of co-released inhibitory transmitters at central synapses. *J Neurosci* 25: 6490–6498, 2005.
- Fink KB, Gothert M. 5-HT receptor regulation of neurotransmitter release. *Pharmacol Rev* 59: 360–417, 2007.
- Ghijsen WE, Leenders AG. Differential signaling in presynaptic neurotransmitter release. *Cell Mol Life Sci* 62: 937–954, 2005.
- Gracheva EO, Burdina AO, Touroutine D, Berthelot-Grosjean M, Parekh H, Richmond JE. Tomosyn negatively regulates both synaptic transmitter and neuropeptide release at the *C. elegans* neuromuscular junction. *J Physiol* 585: 705–709, 2007.
- Hammalund M, Watanabe S, Schuske K, Jorgensen EM. CAPS and syntaxin dock dense core vesicles to the plasma membrane in neurons. *J Cell Biol* 180: 483–491, 2008.
- Heinzel HG, Weimann JM, Marder E. The behavioral repertoire of the gastric mill in the crab, *Cancer pagurus*: an in situ endoscopic and electrophysiological examination. *J Neurosci* 13: 1793–1803, 1993.
- Jan LY, Jan YN. Peptidergic transmission in sympathetic ganglia of the frog. *J Physiol* 327: 219–246, 1982.
- Katz PS, Eigg MH, Harris-Warrick RM. Serotonergic/cholinergic muscle receptor cells in the crab stomatogastric nervous system. I. Identification and characterization of the gastropyloric receptor cells. *J Neurophysiol* 62: 558–570, 1989.
- Kiehn O, Harris-Warrick RM. Serotonergic stretch receptors induce plateau properties in a crustacean motor neuron by a dual-conductance mechanism. *J Neurophysiol* 68: 485–495, 1992.
- Kilman VL, Marder E. Ultrastructure of the stomatogastric ganglion neuropil of the crab, *Cancer borealis*. *J Comp Neurol* 374: 362–375, 1996.
- Kirby MS, Nusbaum MP. Peptide hormone modulation of a neuronally modulated motor circuit. *J Neurophysiol* 98: 3206–3220, 2007.
- Koh HY, Vilim FS, Jing J, Weiss KR. Two neuropeptides colocalized in a command-like neuron use distinct mechanisms to enhance its fast synaptic connection. *J Neurophysiol* 90: 2074–2079, 2003.
- Koh HY, Weiss KR. Activity-dependent peptidergic modulation of the plateau-generating neuron B64 in the feeding network of *Aplysia*. *J Neurophysiol* 97: 1862–1867, 2007.
- Lamotte d'Incamps B, Ascher P. Four excitatory postsynaptic ionotropic receptors coactivated at the motoneuron–Renshaw cell synapse. *J Neurosci* 28: 14121–14131, 2008.
- Lu T, Rubio ME, Trussell LO. Glycinergic transmission shaped by the corelease of GABA in a mammalian auditory synapse. *Neuron* 57: 524–535, 2008.
- Maher BJ, Westbrook GL. Co-transmission of dopamine and GABA in periglomerular cells. *J Neurophysiol* 99: 1559–1564, 2008.
- Marder E. Neurotransmitters and neuromodulators. In: *The Crustacean Stomatogastric System*, edited by Selverston AI, Moulins M. Berlin: Springer-Verlag, 1987, p. 263–300.
- Marder E, Bucher D. Understanding circuit dynamics using the stomatogastric nervous system of lobsters and crabs. *Annu Rev Physiol* 69: 291–316, 2007.
- Nadim F, Manor Y, Nusbaum MP, Marder E. Frequency regulation of a slow rhythm by a fast periodic input. *J Neurosci* 18: 5053–5067, 1998.
- Nishimaru H, Restrepo CE, Ryge J, Yanagawa Y, Kiehn O. Mammalian motor neurons corelease glutamate and acetylcholine at central synapses. *Proc Natl Acad Sci USA* 102: 5245–5249, 2005.
- Norris BJ, Coleman MJ, Nusbaum MP. Pyloric motor pattern modification by a newly identified projection neuron in the crab stomatogastric nervous system. *J Neurophysiol* 75: 97–108, 1996.
- Nusbaum MP, Beenhakker MP. A small-systems approach to motor pattern generation. *Nature* 417: 343–350, 2002.
- Nusbaum MP, Blitz DM, Swensen AM, Wood D, Marder E. The roles of co-transmission in neural network modulation. *Trends Neurosci* 24: 146–154, 2001.
- Ohnuma K, Whim MD, Fetter RD, Kaczmarek LK, Zucker RS. Presynaptic target of Ca<sup>2+</sup> action on neuropeptide and acetylcholine release in *Aplysia californica*. *J Physiol* 535: 647–662, 2001.
- Peng YY, Zucker RS. Release of LHRH is linearly related to the time integral of presynaptic Ca<sup>2+</sup> elevation above a threshold level in bullfrog sympathetic ganglia. *Neuron* 10: 465–473, 1993.
- Prinz AA, Abbott LF, Marder E. The dynamic clamp comes of age. *Trends Neurosci* 27: 218–224, 2004.
- Rudomin P. In search of lost presynaptic inhibition. *Exp Brain Res* 196: 139–151, 2009.
- Saideman SR, Blitz DM, Nusbaum MP. Convergent motor patterns from divergent circuits. *J Neurosci* 27: 6664–6674, 2007.
- Seal RP, Edwards RH. Functional implications of neurotransmitter corelease: glutamate and GABA share the load. *Curr Opin Pharmacol* 6: 114–119, 2006.
- Sharp AA, O'Neil MB, Abbott LF, Marder E. The dynamic clamp: artificial conductances in biological neurons. *Trends Neurosci* 16: 389–394, 1993.
- Sieburth D, Madison JM, Kaplan JM. PKC-1 regulates secretion of neuropeptides. *Nat Neurosci* 10: 49–57, 2007.

- Skiebe P, Schneider H.** Allatostatin peptides in the crab stomatogastric nervous system: inhibition of the pyloric motor pattern and distribution of allatostatin-like immunoreactivity. *J Exp Biol* 194: 195–208, 1994.
- Speese S, Petrie M, Schuske K, Ailion M, Ann K, Iwasaki K, Jorgensen EM, Martin TF.** UNC-31 (CAPS) is required for dense-core vesicle but not synaptic vesicle exocytosis in *Caenorhabditis elegans*. *J Neurosci* 27: 6150–6162, 2007.
- Spitzer N, Edwards DH, Baro DJ.** Conservation of structure, signaling and pharmacology between two serotonin receptor subtypes from decapod crustaceans, *Panulirus interruptus* and *Procambarus clarkii*. *J Exp Biol* 211: 92–105, 2008.
- Stein W, DeLong ND, Wood DE, Nusbaum MP.** Divergent co-transmitter actions underlie motor pattern activation by a modulatory projection neuron. *Eur J Neurosci* 26: 1148–1165, 2007.
- Sun QQ, Baraban SC, Prince DA, Huguenard JR.** Target-specific neuropeptide Y-ergic synaptic inhibition and its network consequences within the mammalian thalamus. *J Neurosci* 23: 9639–9649, 2003.
- Thirumalai V, Marder E.** Colocalized neuropeptides activate a central pattern generator by acting on different circuit targets. *J Neurosci* 22: 1874–1882, 2002.
- Vilim FS, Cropper EC, Price DA, Kupfermann I, Weiss KR.** Peptide cotransmitter release from motoneuron B16 in *Aplysia californica*: costorage, corelease, and functional implications. *J Neurosci* 20: 2036–2042, 2000.
- Watson A, Le Bon-Jego M, Cattaert D.** Central inhibitory microcircuits controlling spike propagation into sensory terminals. *J Comp Neurol* 484: 234–248, 2005.
- Weimann JM, Meyrand P, Marder E.** Neurons that form multiple pattern generators: identification and multiple activity patterns of gastric/pyloric neurons in the crab stomatogastric system. *J Neurophysiol* 65: 111–122, 1992.
- Wood DE, Nusbaum MP.** Extracellular peptidase activity tunes motor pattern modulation. *J Neurosci* 22: 4185–4195, 2002.
- Wood DE, Stein W, Nusbaum MP.** Projection neurons with shared cotransmitters elicit different motor patterns from the same neural circuit. *J Neurosci* 20: 8943–8953, 2000.